

Discrete-Time $\mathcal{H}_2/\mathcal{H}_\infty$ Control of an Acoustic Duct: Delta-Domain Design and Experimental Results

R. Scott Erwin and Dennis S. Bernstein *

Department of Aerospace Engineering, The University of Michigan
Ann Arbor, MI 48109-2118

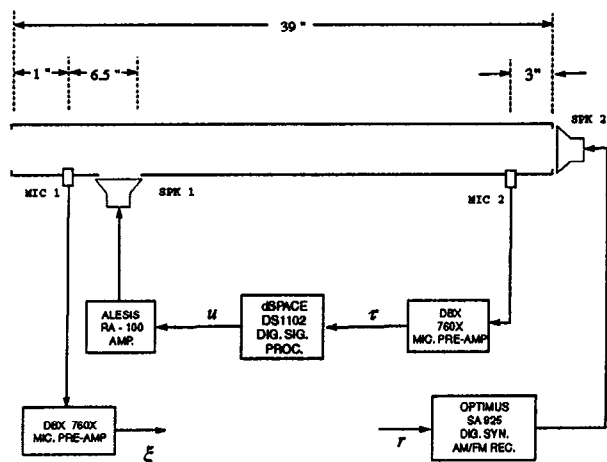


Figure 1: Experimental Configuration

1 Experiment Description

A dimensioned diagram of the experimental configuration of the acoustic duct is shown in Figure 1. The duct is constructed of 4 inch diameter PVC plastic piping. Electret condenser microphones are used as sensors. These omnidirectional microphones measure acoustic pressure and have an approximately flat frequency response over a frequency range of 20 Hz–20 kHz. Acoustic actuation for both disturbance and control was provided by 4" woofer speakers, which have a flat response range of approximately 50 Hz–7 kHz. For control purposes, the inputs r and u are the input voltages to the disturbance and control speaker amplifiers, respectively, while the measurement signals τ and ξ are the output voltages from the measurement and performance microphone amplifiers, respectively. In this way, the combined dynamic characteristics of the amplifiers, speakers, and microphones can be identified directly from experimental data. Controllers are implemented using a dSPACE model DS1102 real-time control board.

2 Model Identification

A Scientific Atlanta SA 390 spectrum analyzer was used to produce averaged sampled frequency response estimates for the four transfer functions between the

*This research was supported by the Air Force Office of Scientific Research under grant F49620-95-1-0019 and the USAF Phillips Laboratory.

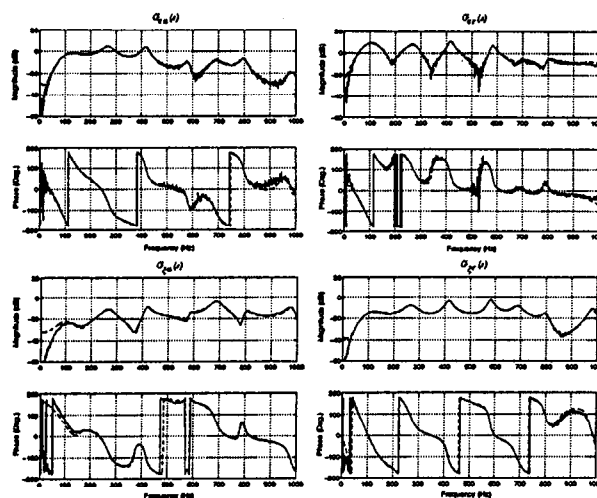


Figure 2: Measured and Identified Frequency Response Functions, 24th-order Identified Model. Solid Line: Measured, Dashed Line: Identified Model.

inputs u and r to the outputs τ and ξ . An approximate impulse response sequence was then generated for each of the four averaged sampled frequency response estimates, and these were combined within the eigen-system realization algorithm (ERA) [3]. This discrete-time model was then converted to the continuous-time counterpart using the inverse impulse-invariant transformation. After several iterations on the model order, a 24th-order model was found to fit the measured frequency responses adequately. A comparison of the identified 24th-order model frequency response functions and their measured counterparts is shown in Figure 2.

3 Control Design Problem and Synthesis

The sound pressure level (SPL) at a given location is related to the RMS acoustic pressure fluctuation at that location. A standard interpretation of the \mathcal{H}_2 norm is the RMS value of the output signal when the system is driven by a white noise process. Thus, \mathcal{H}_2 -optimal control is well-suited to providing acoustic suppression of broad-band disturbances. Robust stability is enforced by incorporating an \mathcal{H}_∞ constraint within the optimal control problem. We assume an addi-

	$\ G_{zw}\ _2$	$\ G_{ed}\ _\infty$
Open-Loop System	10.94	0
Full-order (24th-Order) \mathcal{H}_2	1.536	3.416
2nd-Order \mathcal{H}_2	6.146	1.848
4th-Order \mathcal{H}_2	3.898	3.103
6th-Order \mathcal{H}_2	3.747	4.124
8th-Order \mathcal{H}_2	2.906	3.777
2nd-Order $\mathcal{H}_2/\mathcal{H}_\infty$	6.193	1.000
4th-Order $\mathcal{H}_2/\mathcal{H}_\infty$	4.394	1.000
6th-Order $\mathcal{H}_2/\mathcal{H}_\infty$	4.354	1.000
8th-Order $\mathcal{H}_2/\mathcal{H}_\infty$	3.931	1.000

Table 1: Controller Properties

tive uncertainty model of the form $G_{\tau u, \text{measured}}(j\omega) = G_{\tau u, \text{nominal}}(j\omega) + \Delta(j\omega)$. To account for the frequency dependence of the uncertainty, a model error weighting function $W_2(s)$ is chosen such that $|\Delta(j\omega)| \leq |W_2(j\omega)|$, $0 < \frac{\omega}{2\pi} < 1000$. The resulting augmented system, denoted $G(s)$, is of 25th order. To minimize the effects of aliasing, a sampling frequency of $f_s = 4000$ Hz was used for controller implementation. For discrete-time controller synthesis, the discrete-time difference operator zero-order-hold equivalent of $G(s)$ [4] is computed using this sampling frequency.

Fixed-structure \mathcal{H}_2 and mixed $\mathcal{H}_2/\mathcal{H}_\infty$ controllers were obtained using the synthesis techniques developed in [1, 2] for 2nd-, 4th-, 6th-, and 8th-order controllers. The full-order (24th-order) Riccati-equation based \mathcal{H}_2 -optimal controller for the nominal identified duct model was also synthesized for comparison. Table 1 lists the closed-loop properties achieved by these controllers.

4 Experimental Results

Figure 3 shows simulated and experimentally measured open- and closed-loop frequency response functions from disturbance input r to performance microphone ξ for the 2nd-order \mathcal{H}_2 controller (top) and the 2nd-order $\mathcal{H}_2/\mathcal{H}_\infty$ controller (bottom). The simulated results were based on the nominal 24th-order identified model. Figure 4 presents the same data for the 8th-order \mathcal{H}_2 and $\mathcal{H}_2/\mathcal{H}_\infty$ controllers, respectively. The experimental results show that the simulated attenuation levels are not achieved, and that, for the 8th-order controllers, the lack of robustness of the \mathcal{H}_2 -optimal controllers actually generates an amplification of the open-loop response at several frequencies within the control bandwidth of 20–1000 Hz. We note that the 2nd-order \mathcal{H}_2 controllers do not exhibit the amplification seen in the 8th-order \mathcal{H}_2 controller results, which suggests that the low complexity of this controller may provide some measure of inherent robustness.

References

[1] R. S. Erwin and D. S. Bernstein. Fixed-structure discrete-time \mathcal{H}_2 -optimal controller synthesis using the delta-operator. In *Proc. Amer. Contr. Conf.*, pages 3185–3189, Albuquerque, NM, June 1997.

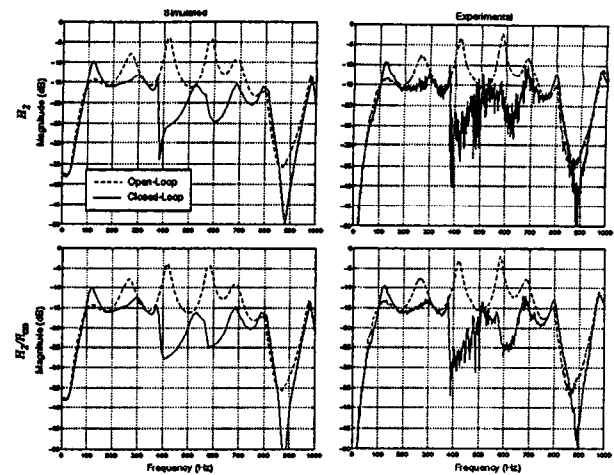


Figure 3: Simulated (left) and Experimental (right) Open- and Closed-Loop Frequency Response Functions, 2nd-order \mathcal{H}_2 Controller (top) and 2nd-order $\mathcal{H}_2/\mathcal{H}_\infty$ Controller (bottom)

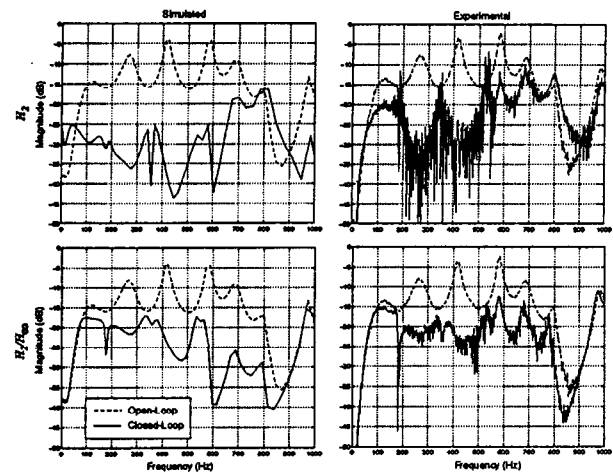


Figure 4: Simulated (left) and Experimental (right) Open- and Closed-Loop Frequency Response Functions, 8th-order \mathcal{H}_2 Controller (top) and 8th-order $\mathcal{H}_2/\mathcal{H}_\infty$ Controller (bottom)

[2] R. S. Erwin and D. S. Bernstein. Fixed-structure discrete-time mixed $\mathcal{H}_2/\mathcal{H}_\infty$ controller synthesis using the delta-operator. In *Proc. Amer. Contr. Conf.*, pages 3526–3530, Albuquerque, NM, June 1997.

[3] J. Juang and R. Pappa. An eigensystem realization algorithm for modal parameter identification and model reduction. *AIAA J. Guid. Contr. Dyn.*, 8:620–627, 1985.

[4] R. H. Middleton and G. C. Goodwin. *Digital Control and Estimation: A Unified Approach*. Prentice-Hall, Englewood Cliffs, NJ, 1990.